J Comput Neurosci (2006) 21:343–357
DOI 10.1007/s10827-006-9082-x

How do glutamatergic and GABAergic cells contribute to synchronization in the medial septum?

Balázs Ujfalussy · Tamás Kiss

Received: 16 February 2006 / Revised: 9 May 2006 / Accepted: 10 May 2006 / Published online: 28 July 2006

Abstract The medial septum-diagonal band (MSDB) complex is considered as a pacemaker for the hippocampal theta rhythm. Identification of the different cell types, their electrophysiological properties and their possible function in the generation of a synchronized activity in the MSDB is a hot topic. A recent electro-physiological study showed the presence of two antiphasically firing populations of parvalbumin containing GABAergic neurons in the MSDB. Other papers described a network of cluster-firing glutamatergic neurons, which is able to generate synchronized activity in the MSDB. We propose two different computer models for the generation of synchronized population theta oscillation in the MSDB and compare their properties. In the first model GABAergic neurons are intrinsically theta periodic cluster-firing cells; while in the second model GABAergic cells are fast-firing cells and receive periodic input from local glutamatergic neurons simulated as cluster-firing cells. Using computer simulations we show that the GABAergic neurons in both models are capable of generating antiphasic theta periodic population oscillation relying on local, septal mechanisms. In the first model antiphasic theta synchrony could emerge if GABAergic neurons form two populations preferentially innervate each other. In the second model in-phase synchronization of glutamatergic neurons does not require specific network structure, and the network of these cells are able to act as a theta pacemaker for the local fast-firing GABAergic circuit. Our simulations also suggest that neurons being non-cluster-firing *in vitro* might exhibit clustering properties when connected into a network *in vivo*.

Keywords Theta · Cluster-firing · Fast-firing · Network structure · Preferred firing phase

Action Editor: David Golomb

B. Ujfalussy (✉) · T. Kiss
Department of Biophysics, KFKI Research Institute of the Hungarian Academy of Sciences 29–33 Konkoly-Thege street, H-1121 Budapest, Hungary
e-mail: ubi@rmki.kfki.hu

B. Ujfalussy · T. Kiss
Center for Complex Systems Studies, Kalamazoo College, Kalamazoo, MI 49006

1. Introduction

The medial septum-diagonal band (MSDB) complex is believed to play a crucial role in the generation and maintenance of a typical hippocampal oscillatory activity the temporally nested theta (4–12 Hz) and gamma (40–60 Hz) rhythm (Petsche et al., 1962; Stewart and Fox, 1990; Vinogradova, 1995). The hippocampal theta oscillation, which is a large amplitude coherent oscillation, prominent during immobility and exploratory movements (Vanderwolf,1969; Vértes and Kocsis, 1997) is fundamental in several neural computations like memory formation (Hasselmo et al., 2002) and memory related tasks, such as navigation (O'keefe and Nodel, 1978) in many different ways (Lengyel et al., 2005).

Classically, neurons in the MSDB were considered either cholinergic or GABAergic based on their different anatomical and electro-physiological properties (Brashear et al., 1986; Griffith, 1988; Kiss et al., 1990). GABAergic cells interconnected via axo-somatic synapses (Henderson et al., 2004) innervate different hippocampal interneurons (Freund and Antal, 1988) driving them by firing rhythmic bursts phase locked to the hippocampal theta rhythm (Green and Arduini, 1954; Bland et al., 1999; Brazhnik and Fox, 1997; Stewart and Fox, 1990). Cholinergic cells also display rhythmic burst-firing activity (Brazhnik and Fox, 1997, 1999), but they

have slower modulatory effect than GABAergic cells (Cole and Nicoll, 1984) and they innervate both interneurons and pyramidal cells in the hippocampus (Frotscher and Leranth, 1985). By analyzing the phase relationship between medial septal unit activity and hippocampal field oscillation a strong phase coupling was observed both in anaesthetized (Brazhnik and Fox, 1997) and in freely moving rats (King et al., 1998; Dragoi et al., 1999; Brazhnik and Fox, 1999), but the preferred firing phase of different cell types remained unclear. A recent study used combined immunocytochemical and electro-physiological methods to demonstrate that parvalbumin expressing (PV+), GABAergic cells show bimodal phase distribution during hippocampal theta activity (Borhegyi et al., 2004). *In vitro* studies on MSDB neurons showed that GABAergic cells express parvalbumin and exhibit fast-spiking activity (Morris et al., 1999; Sotty et al., 2003).

The first neuron type found to exhibit sustained rhythmic activity *in vitro* was a cluster-firing cell type described by Serafin et al. (1996). These neurons were considered as non-cholinergic, putative GABAergic neurons. Later, Sotty et al. (2003) using simultaneous electro-physiological and biochemical methods identified them as glutamatergic neurons. The presence of a population of glutamatergic neurons in the MSDB has been recently confirmed by anatomical studies (Hajszan et al., 2004; Colom et al., 2005). These glutamatergic neurons form a network that is able to produce slow, synchronized bursting activity and innervate local GABAergic and cholinergic cells (Manseau et al., 2005). A recent *in vitro* study also showed that activation of glutamate receptors can synchronize MSDB neurons in theta frequency (Garner et al., 2005).

The aim of the present study is (i) to determine how theta synchronized bursting activity can emerge internally within the MSDB in a network of GABAergic neurons and (ii) how the bimodal preferred firing phase distribution (Bor-hegyi et al., 2004) of these cells is generated. To achieve this, two competing models will be set up and compared based on competing experimental results. In the first model, which will be referred to as the "ping-pong model", GABAergic cells are modeled as cluster-firing cells (Serafin et al., 1996), which form two subpopulations (SPs) preferentially innervating each-other. In the ping-pong model no other cell type is simulated explicitly. In the second model, which will be referred to as the "feed-forward model" both glutamatergic and GABAergic cells are simulated. In this model, contrary to the ping-pong model, GABAergic cells are of the fast-firing type (Morris et al., 1999) and glutamatergic cells producing their phasic drive are modeled as cluster-firing neurons (Sotty et al., 2003). In the following sections the two models are described in detail and studied to identify characteristic properties suitable for experimental validation.

2. Methods

2.1. Neuron models

Two types of neurons were simulated in the present study: a cluster-firing and a fast-firing neuron. Details of the model equations can be found in the Appendix.

Cluster-firing neuron. To model cluster-firing neurons in the MSDB we used the single compartment model described by Wang (2002) with unchanged parameters unless otherwise noted. This model contains spike generating currents (I_{Na}, I_K)and a slowly inactivating potassium current (I_{KS}). The membrane potential change is given by the following current balance equation:

$$C_m dV/dt = -I_{Na} - I_K - I_{KS} - I_L - I_{syn} + I_{ext} \quad (1)$$

where $C_m = 1\,\mu F/cm^2$ is the membrane capacitance, I_L is the leakage and I_{syn} is the synaptic current. I_{ext}, the external current, is a constant depolarizing current representing background excitation mostly due to cholinergic innervation. The membrane noise term, originally introduced by Wang was omitted. For numerical integration of these equations the initial membrane potential of each cell was chosen randomly from a Gaussian distribution of mean $\mu(V_{init}) = -64$ mV and standard deviation $\sigma(V_{init}) = 30$ mV. The external current of this cell type was also taken from a Gaussian distribution. In the case when cluster-firing cells represented GABAergic neurons (the ping-pong model) the external current was set to $\mu(I_{ext}) = 0.025$ nA, $\sigma(I_{ext}) = 0.0025$ nA mean and standard deviation, respectively. When cluster-firing neurons represented glutamatergic cells (the feed-forward model) the external current was set to a slightly smaller value in order to achieve population oscillation frequency around 5 Hz ($\mu(I_{ext}) = 0.02$ nA, $\sigma(I_{ext}) = 0.002$ nA mean and std, respectively). In control conditions an individual cell fires clusters of action potentials in the theta frequency range (4–6 Hz) while the intracluster frequency is in the gamma range (40–50 Hz, 1A, inset).

In order to gain more insight into the model's functioning we prepared the bifurcation diagram of the model. The single cell model can be considered as a five dimensional dynamical system with dynamical variables V, the membrane potential; h gate of the sodium channel; n gate of the delayed rectifier potassium channel; p and q gates of the slow potassium channel. Since the time constant of the q gate is one order longer (∼100 ms) than that of all other variables, this gate controls the bursting behavior of the cell. When the activation of the q gate was varied as a parameter (reduced, 4 dimensional model) to identify its contribution to the evolution of the membrane potential a subcritical Hopf bifurcation

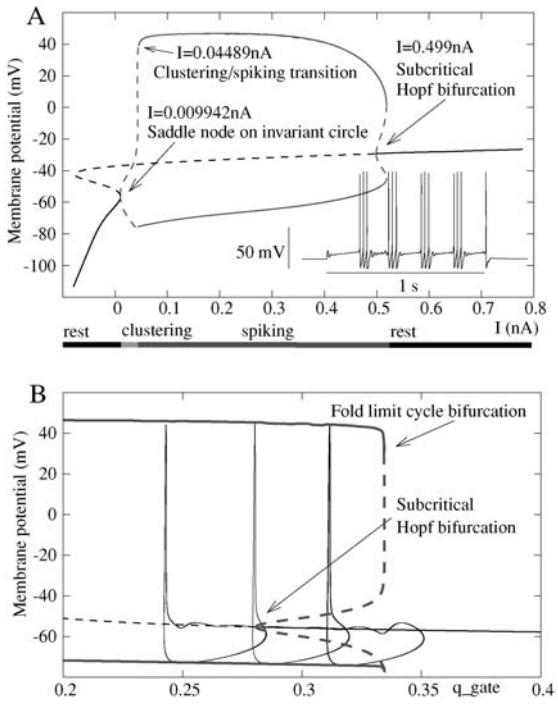

Fig. 1 The slow potassium channel governs the cluster-firing of the model neuron. A: Bifurcation diagram of the cluster-firing neuron. Increasing the applied current the stable equilibrium point disappears, an unstable periodic orbit emerges and the cell fires clusters of action potentials ($0.001 < I_{\text{ext}} < 0.045nA$). Further increasing the applied current stabilizes the periodic orbit and the neuron fires regular spikes with high frequency. The neuron has a second equilibrium at large positive currents. (black line: stable fixed point, black dashed line: unstable fixed point, gray line: stable periodic orbit, gray dashed line: unstable fixed point) The inset shows the response of the neuron to an $I = 0.025$ nA current pulse. B: Bifurcation diagram of the reduced (four dimensional) model. The activation of the q gate is the bifurcation parameter. Trajectory (black line) of the five dimensional model is projected to the q–V plane. Activation and inactivation of the dynamical variable q governs the cluster-firing behavior. When the q gate is open, the system has a single and stable fixed point attractor (resting state). Since its steady-state value is small at the resting state the q gate starts to close, the fixed point becomes unstable and a periodic orbit emerges via a Hopf bifurcation. The system diverges from the unstable fixed point to a stable oscillation (spiking state). Due to the long AHPs, the average membrane potential is more negative during the spiking state and the q gate opens slowly. This increase in the conductance of the slow potassium current terminates the spiking

was found to separate the resting and the spiking state of the model (Fig. 1B). The other four dynamical variables belong to the fast subsystem responsible for the spiking behavior and the subthreshold oscillation. In the simulations we used the original, 5 dimensional model, the bifurcation analysis was made to gain more insight into the model's functioning and the reduced model was not used later in our simulations.

Fast-firing neuron. Medial septal fast-firing, non accommodating neurons were shown to express parvalbumin (Morris et al., 1999), a calcium binding protein, suggesting that these neurons are GABAergic and project to the hippocampus (Freund, 1989).

To model these neurons we simplified the cluster-firing neuron model used in Wang (2002), described briefly in the previous section, by omitting the slow potassium channel, which is responsible for the cluster-firing behavior. The speed of the inactivation of I_{Na} and the activation of I_{K} were increased by changing the temperature factor ϕ from 5 to 10 so that the AHPs became smaller. The membrane potential change of the fast-firing cell is given by the following current balance equation:

$$C_{\text{m}}\text{d}V/\text{d}t = -I_{\text{Na}} - I_{\text{K}} - I_{\text{L}} - I_{\text{syn}} + I_{\text{ext}} \tag{2}$$

To introduce heterogeneity the initial membrane potential of each cell was chosen from a Gaussian distribution of mean $\mu(V_{\text{init}}) = -64$ mV and standard deviation $\sigma_{V_{\text{init}}} = 30$ mV. The I_{ext} background current was an important parameter for synchronization of these neurons and were varied between $\mu(I_{\text{ext}}) = -0.008$ nA and $\mu(I_{\text{ext}}) = -0.026$ nA. The basic behavior of this model (Fig. 6B) is similar to physiological measurements from fast firing cells, except that the model lacks the depolarizing sag and spike frequency adaptation, which is present in most of the GABAergic cells in the MSDB (Sotty et al., 2003).

2.2. Synapse models

Two types of synapses were simulated:

GABAergic synapse model. GABA_{A} IPSCs were described based on (Wang and Buzsáki, 1996) by the equation:

$$I_{\text{syn}} = \bar{g}_{\text{syn}} s(V - E_{\text{syn}}), \tag{3}$$

where $\bar{g}_{\text{syn}}$ is the maximal synaptic conductance, and the activation variable s was governed by the following first order kinetics:

$$\frac{\text{d}s}{\text{d}t} = \alpha F(V_{\text{pre}})(1 - s) - \beta s, \tag{4}$$

where the transmitter release probability $F(V_{\text{pre}})$ was a function of the membrane potential of the presynaptic neuron:

$$F(V_{\text{pre}}) = \frac{1}{1 + \exp\left(-\frac{V_{\text{pre}} - \Theta_{\text{syn}}}{K}\right)} \tag{5}$$

Parameters characterizing synaptic contacts between different pre- and postsynaptic neurons were as follows: $\alpha = 14$ ms^{-1}, $\beta = 0.07$ ms^{-1}, $K = 2$ mV, $\Theta_{\text{syn}} = 0$ mV, $E_{\text{syn}} = -75$ mV. The synaptic conductance was set

to $g_{syn} = 0.25$ nS when GABAergic cells are modeled as cluster-firing cells or $g_{syn} = 0.189$ nS when they were fast-firing neurons. We set the synaptic conductances differently to compensate for the different current–frequency relationship of the two model neurons and to obtain similar IPSP amplitudes.

Glutamatergic synapse model. Glutamatergic transmission was mediated by AMPA receptors described in Destexhe (2000). Briefly

$$I_{AMPA} = \bar{g}_{AMPA} s(V - E_{AMPA}) \tag{6}$$

$$\frac{ds}{dt} = \alpha[T(V_{pre})](1 - s) - \beta s \tag{7}$$

Here, $\alpha = 1.1$ mM^{-1}ms^{-1}, $\beta = 0.19$ ms^{-1}, $E_{AMPA} = 0$ mV, $g_{AMPA} = 0.1$nS on glutamatergic and $g_{AMPA} = 0.15$nS on GABAergic cells. The concentration of the released transmitter ($[T(V_{pre})]$) is a function of the presynaptic membrane potential,

$$[T(V_{pre})] = \frac{T_{max}}{1 + \exp\left(-\frac{V_{pre} - \Theta syn}{K}\right)}, \tag{8}$$

where $T_{max} = 1$ mM, $\Theta_{syn} = 2$ mV, and $K = 5$ mV.

2.3. Network models

Recent physiological findings (Henderson et al., 2004, Borhegyi et al., 2004) suggest that a delicate synaptic connection pattern might account for the pacemaker capability of septal GABAergic cells. It was shown that the distribution of preferred firing phases of medial septal PV+ GABAergic neurons is a bimodal distribution: a subpopulation of these cells preferentially fire at the peak while the other SP at the trough of the hippocampal field theta oscillation (Borhegyi et al., 2004). This experimental finding encouraged us to examine the role of the connectivity between and within the two GABAergic SPs in the synchronization of MSDB neurons.

In the following sections two models will be introduced and studied. In the first model, the ping-pong model, only GABAergic neurons were simulated. Here GABAergic neurons are described as cluster-firing cells. These cells were divided into two SPs. Connection probabilities $p_{AA}, p_{AB}, p_{BA}, p_{BB}$ are defined to give the probability of connecting two neurons chosen from SP A or one from SP A to one from SP B, etc., respectively, using the $GABA_A$ synapse model. Connection probability between two cells from the same (different) SP(s) is described by $p_{AA} = p_{BB} = p_c - b$ ($p_{AB} = p_{BA} = p_c + b$), respectively, where p_c is the connection probability in the whole network and b means the bias (or polarization parameter) to preferentially innervate neurons from the other SP. The value of b was systematically varied between 0 and 0.5 while p_c was kept constant. If b is low (around zero) then the network has random connectivity (Fig. 2A); if, on the other hand, b is high then the network is divided into two SPs reciprocally innervating each other (a polarized network, Fig.2B). Autapses were not allowed. Each of the SPs contained 20 neurons. No other neuron types (cholinergic or glutamatergic) were simulated in the ping-pong model.

The second network presented here, the feed-forward model, consisted of both glutamatergic and GABAergic neurons. Glutamatergic neurons were described as cluster-firing cells, GABAergic neurons as fast-firing cells. The GABAergic network again was divided into two subpopulations as described above. Glutamatergic cells randomly innervated neurons of only one of the two GABAergic subpopulation by AMPA receptor mediated synapses with probability $p_{UA} = 0.5$. In this model only glutamatergic and GABAergic neurons were simulated, the tonic effect of cholinergic neurons was implicitly taken into account by the I_{ext} external current. We simulated 40 glutamatergic and 40 GABAergic neurons in the feed-forward model.

In order to analyze the effect of heterogeneity introduced to the system we made 10 parallel simulations with different connection matrices and initial conditions.

2.4. Softwares and mathematical analysis

The bifurcation diagrams were prepared using the XPPAUT (version: 5.91) simulation environment (Ermentrout, 2002), all other simulations were performed using the GENESIS (version 2.2) software package (Bower and Beeman, 1998) under the Linux operating system. Mathematical analysis of the results were performed using the GNU octave (version 2.1.69).

To quantify the synchronization of the neuronal firing in the network, we introduced a coherence index based on the correlation between the activity of cell pairs from the same network. The activity of each cell was defined by dividing the simulation time T into small bins of τ width and the value of a given bin was 1 if the cell fired during that interval or 0 if not. Thus, the coherence index of a network is calculated as the mean correlation between the activity of all cell pairs from the network. We calculated gamma coherence with $\tau = 5$ ms and theta coherence with $\tau = 50$ ms.

To define the firing phase of a cell a periodic reference signal was required. Since the hippocampal regions are not included in the simulations we can not relate the firing phase of the individual cells to a hippocampal signal like in experimental studies. Instead, we quantified the relative preferred firing phases of the two GABAergic subpopulations via an arbitrarily chosen reference signal and compared these relative values with experimental findings. In the experiments

by Bor-hegyi et al. (2004) the relative phase difference between the two SPs was approximately 152° corresponding to ∼100–70 ms time difference depending on the theta frequency (4–6 Hz). The reference signal used in our calculations was the mean firing rate versus time function of one of the SPs (Fig. 4C). 0° was chosen to be the trough, 180° the peak of this sinusoid-like signal. Mean firing rate of the SPs was calculated as the mean of its cells' approximate firing rate. The approximate firing rates were calculated by convolving the series of firings by a Gaussian of 1 ms standard deviation according to Dayan and Abbott (2001). The phase (Φ) of each spike was calculated relative to this signal, i.e. the minimum and the maximum between which the spike occurred were identified and the phase of the spike was calculated by

$$\Phi = \begin{cases} 180^\circ \dfrac{t}{t_{\max} - t_{\min}} & \text{if} \quad t_{\max} > t_{\min}, \\ 180^\circ \dfrac{t}{t_{\max} - t_{\min}} + 180^\circ & \text{if} \quad t_{\max} < t_{\min}. \end{cases} \tag{9}$$

where t is the time when the spike was emitted, $t_{\min}$ and $t_{\max}$ are the time of the minimum and the maximum, respectively, of the mean firing rate of the SP. This phase was regarded as a vector of unit length and of angle Φ. The sum of these vectors calculated for all spikes of a cell divided by the number of spikes fired was considered as the preferred firing phase of a given neuron. Mean phases of the two SPs were calculated by taking the average of the phase vectors of a given SP's cells.

We distinguish between the terms *clustering* and *cluster-firing*. The latter means that a cell responds to a constant depolarizing current with repetitive clusters of action potentials. Clustering, on the other hand, means that the firing pattern of a neuron in a network contains clusters of action potentials. The cause of clustering could be both network and/or single-cell phenomena: (i) non-cluster-firing cells when connected into a network or driven by some phasic input might emit spikes in clusters, or (ii) cluster-firing cells in a properly connected network might preserve their cluster-firing property. We say that the ith spike is the first and the jth spike is the last spike of a cluster if (a) the interspike interval before and after the cluster is sufficiently large; (b) the cluster is sufficiently long (there are more than one spike in the cluster); (c) the cluster is not longer than one theta period. Quantitatively:

$$[ISI_{(i-1)}, ISI_j] > 1.5 * \frac{\sum_{k=1}^{n} ISI_k}{n} \tag{10a}$$

$$t_j - t_i > 0.001 \text{ s} \tag{10b}$$

$$t_j - t_i < 0.3 \text{ s} \tag{10c}$$

where ISI_{i} means the ith interspike interval, n is the number of ISIs during the simulation and t_i is the time of the spike before the ith interspike interval. A neuron is considered as a clustering cell if it has on the average more than 3 clusters in 1 s.

Power spectra of network activities were calculated using octave's Fast Fourier Transformation algorithm. Theta (gamma) power were determined as the sum of the power spectrum values between 4–10 (40–80) Hz.

3. Results

Our hypothesis was that the structure of local synaptic connections between GABAergic cells in the MSDB is responsible for their synchronization and for the generation of a preferred firing phase.

We give two different models for theta and gamma synchronization in the medial septum. In the ping-pong model discussed in Section 3.1 GABAergic cells are autonomous theta periodic pacemakers (cluster-firing cells), while in the feed-forward model, studied in Section 3.2, they are fast-firing neurons with external theta-periodic input from the local glutamatergic circuit, in which glutamatergic cells are simulated as cluster-firing neurons.

3.1. Synchronization in a network of cluster-firing GABAergic cells

First, we analyzed the random network of cluster-firing cells, i.e. the ping-pong model with $b = 0$ (Fig. 2A). Wang (2002) showed that spikes of cluster-firing neurons are synchronized in an all-to-all network, while the clusters of the cells were asynchronous. In our model cells in the random network also have synchronized activity. We found that some cells fire clusters of action potentials, while a subset of cells fire single spikes or doublets (Fig. 2C). There is no theta modulation in the population activity of the network as shown by the population activity histogram (Fig. 2C), upper trace) and the FFT (Fig. 2E).

Second, the polarization of the network was increased by increasing the bias (b) parameter in the connection probability (see Methods). In a polarized network theta periodic clusters of action potentials of neurons from one SP alternate with clusters of the other SP and strong theta modulation is present in the activity of both SPs (Fig. 2D, E). On the FFT histograms an other peak at gamma frequency (∼40 Hz) indicates that spikes are also synchronized in the polarized network Fig. (2E).

The proportion of clustering cells (neurons that fire periodic clusters not single spikes; see Methods) in the ping-pong

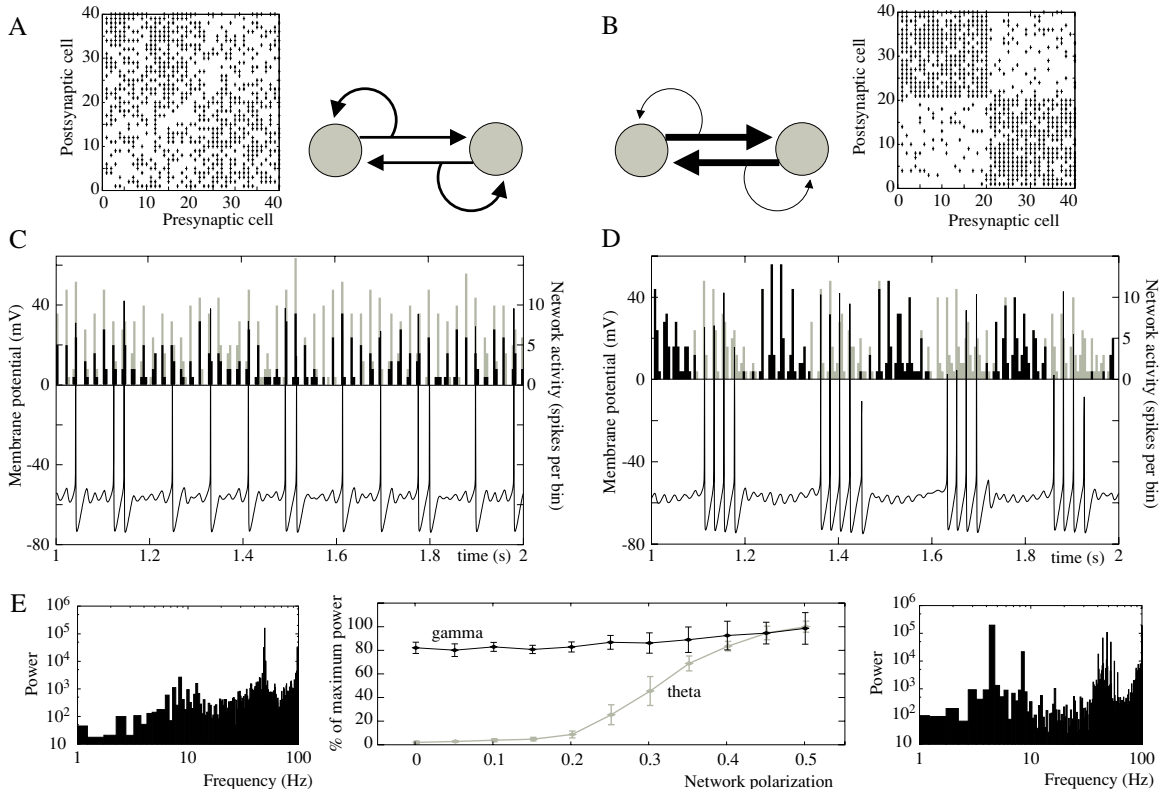

Fig. 2 Network structure and synchronization in the ping-pong model. A: Connection matrix and the schematic diagram shows the structure of a random network. Shaded circles represent subpopulations of cluster-firing neurons, arrows mean GABAergic synaptic connections and the size of the arrow represents the connection probability between cells from the given subpopulation(s). The connection probability between each pair of neurons is the same. B: Connection matrix and schematic diagram of a polarized network. The connection probability between cells from different subpopulations is higher than between cells from the same subpopulation. The total number of synapses are similar in the random and in the polarized networks. C–D: The activity of the two subpopulations (gray bars are drawn above black bars) and the membrane potential of one neuron are shown in the random (C) and in the polarized (D) network. The plotted population activity represents the number of spikes fired by all cells from the given subpopulation in a 5ms long time-bin. In the random network (C) some cells fire single action potentials and the spikes are synchronized to each other (see population activity). In the polarized network (D) neurons fire clusters of action potentials where both the spikes and the clusters are synchronized. The two populations are antiphasic. Notice the fast IPSPs between the spike-clusters. E: Power spectrum of the network activity in the random (left) and the polarized (right) case. The middle panel shows the change of theta and gamma power with network polarization

model rapidly increases with network polarization between bias $b = 0.2$ and $b = 0.3$ (Fig. 3A). Above this critical range (indicated by the shadowed region on Fig. 3) the theta and gamma coherence in the SPs are also high (Fig. 3B, C). The coherence between the two SPs is negative because the two populations are antiphasic. Below the critical range the theta coherence is similar to the control, while the gamma coherence is positive both within and between the SPs.

We tested a larger ($N = 80$) polarized ($b = 0.5$) ping-pong model with sparser synaptic connections to identify what properties of the system determine theta synchronization characteristics. We found that the product of the total number and the strength of synapses arriving to a given cell is critical for theta synchronization (data not shown). A two-fold decrease in the number of synaptic contacts of a cell compensates an increase of similar magnitude in the synaptic strength. In a network of 80 neurons the minimal connection probability required for stable theta synchronization was $p_c \sim 0.2$ (approximately 16 $GABA_A$ synapses converging onto a cell) with a maximal synaptic conductance of $g_{syn} = 0.25$ nS. Similarly, to achieve the same theta synchrony in a network of 40 neurons with $g_{syn} = 0.25$ nS the connection probability was doubled: $p_c \sim 0.4$. The dependence of theta coherence on the network polarization (b) was similar in the large and in the small networks (data not shown).

In symmetric networks clusters of firing of the two SPs are exactly antiphasic (the phase difference is $180 \pm 8^\circ$, Fig. 4A). Neurons from the same SP have slightly different preferred firing phases (Fig. 4A–C) but the preferred firing phase of the neurons was independent of their firing rate (Fig. 4B, correlation between the firing rate and the preferred firing phase in one SP was -0.1 ± 0.2; the mean and the std. of 10 independent simulation).

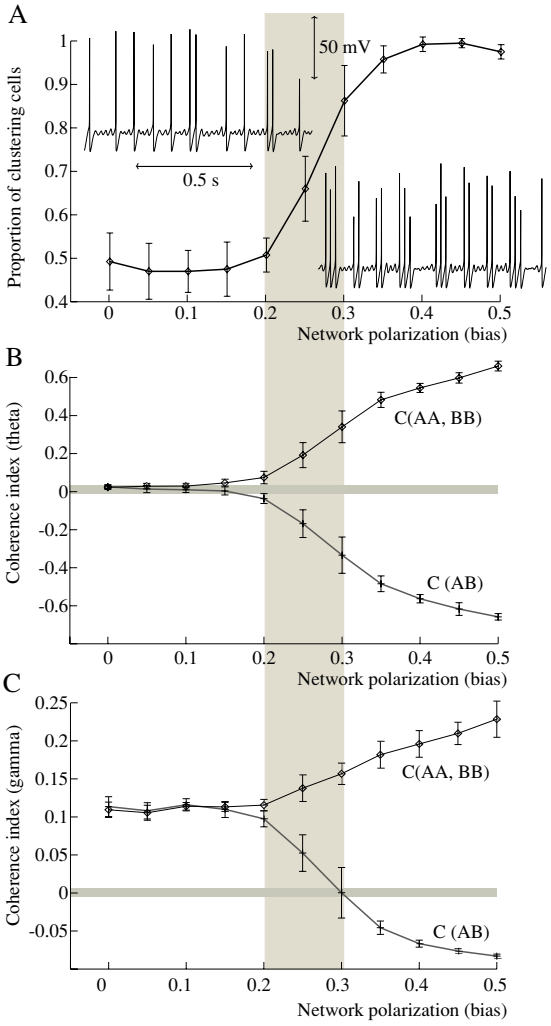

Fig. 3 Antiphasic synchronization characterize networks where the bias is higher than approximately 0.25. A: Proportion of clustering cells in the whole network rapidly increases (from ∼0.5 to ∼1) between bias 0.2 and 0.3 (critical range, indicated by the shadowed box). In a random network (low bias) ∼50% of the cells fire single spikes (left inset), others fire clusters of action potentials (right inset) depending on their external current and synaptic connections. Both insets are taken from the same subpopulation, bias = 0.05. B–C: Theta (B) and gamma (C) coherence of the network also change substantially in the critical range of the bias. The horizontal shaded region shows the mean and the standard error of the correlation between uncoupled cells for control. High negative correlation values between the two subpopulations indicate that they are antiphasic. Spike synchronization (gamma rhythm) is present in the random network. Error bars show the standard deviation of 10 parallel simulations with the same parameters

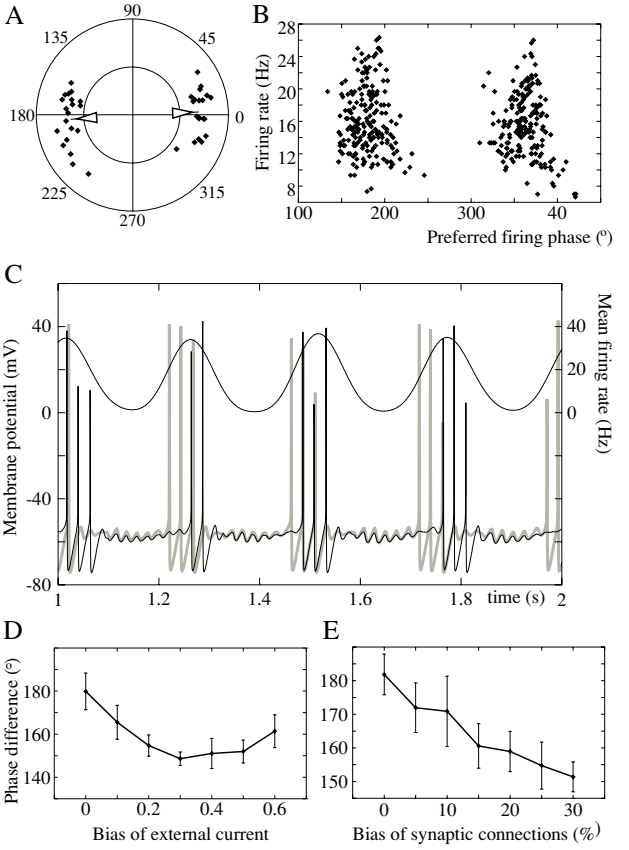

Fig. 4 Phase relationship between GABAergic neurons in the ping-pong model. A: The polar plot shows that the preferred firing phase of neurons related to the mean firing rate of one subpopulation shows a bimodal distribution. The distance from the center corresponds to the vector length (center: 0, periphery: 1; see Methods). Large distance means strong phase preference. B: There is no correlation between the firing rate and the preferred firing phase of the neurons. (400 neurons from 10 parallel simulations are shown). C: Example for two neurons from the same subpopulation with different preferred firing phases (black and gray lines). The phase difference between the two cells is ∼50°. The mean firing rate of one SP (upper black line) is used as reference to calculate the firing phases. D: The phase difference between the two subpopulations is smaller if their external currents are different. Bias is the difference from the mean in μA/cm^2. E: Phase difference between the two subpopulations decreases when synapses are asymmetric: synapses from subpopulation A to B are stronger than synapses from B to A. Bias is the difference from the mean in %. Parameter $b = 0.45$ on this figure

In their experiments Bor-hegyi et al. (2004) found that the phase difference between the two SPs was significantly smaller than 180°. In order to study if our network is able to show smaller phase difference between the two SPs we introduced asymmetry in the ping-pong model by increasing the external current (I_{ext}) applied to one of the SPs while decreasing it to the other. This asymmetry gradually decreased the phase difference between the two SPs (Fig. 4D). Similar result is obtained when the asymmetry was in the synaptic connections between the two SPs (Fig. 4E). However, when the external current or the inhibition is highly unbalanced then one of the two SPs remains silent and the network do not show synchrony.

3.2. Synchronization in a network of fast-firing GABAergic cells

Second, we studied the feed-forward model, which consisted of two SPs of fast-firing GABAergic neurons with theta periodic pacemaker input arriving to only one of the two SPs (Excitatory driven SubPopulation or *ESP*; while the other SP is called Inhibitory driven SubPopulation or *ISP*). In this model theta periodic pacemaker input is generated by a network of glutamatergic neurons (see Section 3.2.1) simulated as cluster-firing cells.

The feed-forward model is motivated by simultaneous electro-physiological and anatomical studies (Sotty et al., 2003; Manseau et al., 2005), which suggest that cluster-firing cells are more likely to be glutamatergic than GABAergic and GABAergic neurons show fast-firing behavior. These glutamatergic cells innervate other local neurons including glutamatergic and GABAergic cells (Manseau et al., 2005). Building on this justification glutamatergic cells in the feed-forward model were simulated as cluster-firing cells.

3.2.1. Glutamatergic neurons act as pacemakers for septal theta rhythm

Glutamatergic cells were described by the cluster-firing cell model and were interconnected into a network by fast glutamatergic synapses (see Methods). The same analysis was conducted for this network as described in Section 3.1 for cluster-firing cells interconnected by GABAergic connections (i.e. systematically increasing the *b* bias parameter) to show that network polarization can not eliminate robust in-phase synchronization in the present case. Simulations show that spikes and clusters of coupled glutamatergic neurons are synchronized to each other (Fig. 5A) and theta or gamma coherence of the network does not change with the polarization (Fig. 5B). Instead of antiphasic synchronization as seen in the ping-pong model, glutamatergic cells show in-phase synchronization since these neurons fire their spikes and clusters simultaneously in the whole network (Fig. 5C, D) and the mean phase of all cells' firing are similar.

This robust in phase synchronization allows the glutamatergic network to be a local theta periodic pacemaker for a network of fast-firing GABAergic neurons in the medial septum.

3.2.2. Theta synchronization in the feed-forward model

The theta periodic input generated by the local glutamatergic network was used to drive GABAergic cells of the feed-forward model. Only neurons from one of the two SPs are innervated by local glutamatergic cells (*ESP* on Fig. 6A,) with connection probability $p_{UA} = 0.5$. The other

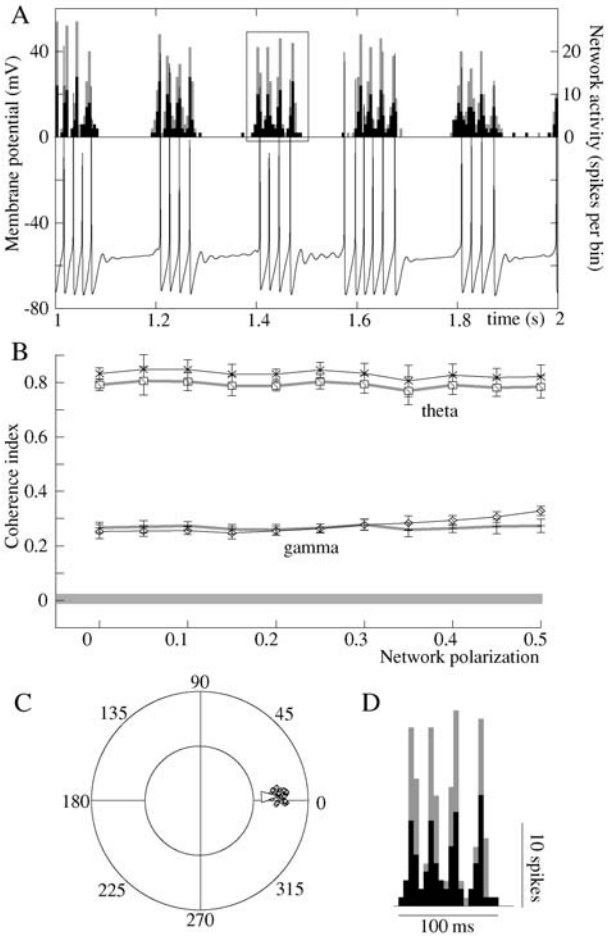

Fig. 5 Synchronized activity in the excitatory network is independent from the network polarization. A: Population activity of the two subpopulations (gray bars are drawn on top of black bars) and the membrane potential of a representative neuron. Action potentials and clusters are synchronized in the whole population. B: The synchrony of the cells does not change with the polarization of the network. Coherence between cells from the same (different) subpopulation(s) are shown by black (gray) lines. Horizontal shaded region shows the mean and the standard error of the correlation between uncoupled cells for control. C: The polar plot shows that the preferred firing phase of the cells are similar (see caption of Fig. 4A). D: Discrete peaks of population activity enlarged from A show that the spikes of the cells are synchronized within the clusters

SP, that lacks glutamatergic innervation (*ISP* on Fig. 6A) needs stronger excitatory current (I_{ext}) to maintain its firing capability, which is decreased by the inhibitory innervation from the ESP. When the fast-firing GABAergic neurons are innervated by the glutamatergic network GABAergic cells from the two SPs fire alternating clusters of action potentials (Fig. 6C, D). As action potential generation is the result of the interplay between their intrinsic dynamics and the glutamatergic innervation the activity of the neurons from the *ESP* is highly irregular. On the other hand, the *ISP* lacks synaptic input during its active state (it is inhibited while the ESP is active and starts firing when disengaged from its

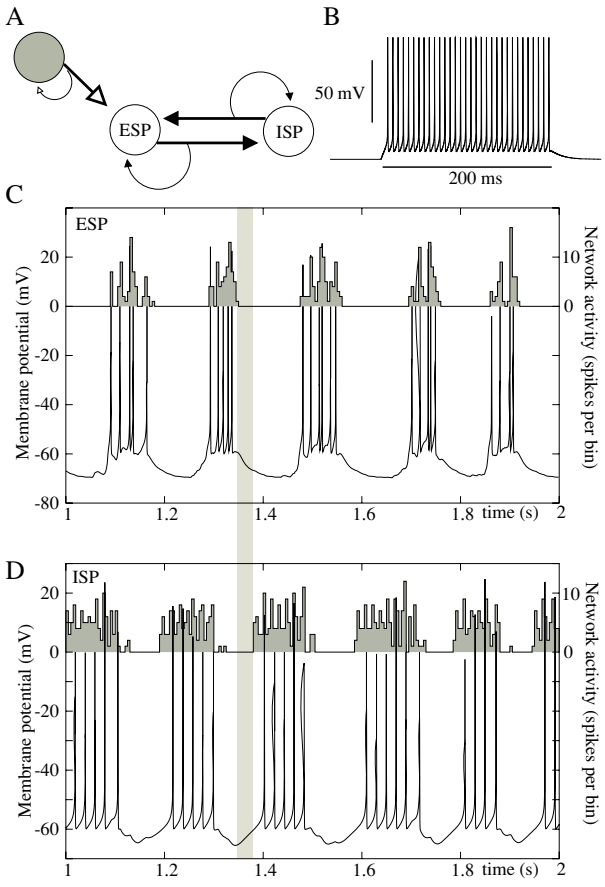

Fig. 6 Interactions between septal glutamatergic and GABAergic neurons: the feed-forward model. A: A randomly interconnected network of glutamatergic neurons innervate a subpopulation (*ESP*) of fast-firing GABAergic cells. The two GABAergic subpopulations reciprocally innervate each other (shaded circle: cluster-firing neuron, open circle: fast-firing neuron, open arrow: glutamatergic connection, filled arrow: GABAergic connection). B: Response of a fast-firing neuron to an external current pulse (dI = 0.025 nA). C–D: Activity of the two GABAergic subpopulations and an example for the membrane potential trace (C, *ESP* and D, *ISP*). The neurons in the two subpopulations fire intermittent clusters like cells in Fig. 2D, but these clusters are driven by EPSPs and IPSPs and not by the cell's intrinsic dynamics. The shaded box shows the delayed firing of the inhibitory driven subpopulation. Parameters: $I_{ext,ESP} = -0.0225$ nA, $I_{ext,ISP} = -0.012$ nA, bias = 0.45

inhibition) so the firing pattern of these neurons is more regular and governed by its membrane dynamics and the tonic drive. The gamma and theta coherence in the GABAergic SPs of the feed-forward model are similar to those seen in the polarized ping-pong model (data not shown).

In the feed-forward model cells from both GABAergic SPs fired in clusters in the whole external current range ($-0.025 \leq I_{ext,ESP} \leq -0.0175$ nA) that enabled firing (Fig. 7A, B) (i.e. when the firing rate of both populations is greater than zero on Fig. 7B). The activity of neurons from the *ESP* were similar in the random (small b) and the polarized ($b \sim 0.5$) networks because of their strong coupling to the local glutamatergic cells (Fig. 7C, D).

Neurons from the *ISP* were antiphasic with the *ESP* in both the random and the polarized networks (Fig. 7G, H), but due to recurrent collaterals more *ISP* neurons had lower firing rate in the random network than in the polarized network (Fig. 7D). Due to these feed-back connections the proportion of clustering *ISP* cells was also smaller in the random case than in the polarized case. Although, the total inhibition arriving to a given neuron is similar in the random and in the polarized networks (because the connection probability (p_c) and thus the mean number of synapses on a given neuron are equal in the two cases) as the two SPs fire intermittently the inhibition in a polarized network is phasic while in a random network it is more tonic.

In a random network the proportion of clustering cells in the *ISP* was smaller than in the *ESP* (Fig. 7C). In this case the tonic inhibition decreases the firing rate of the cells with lower I_{ext} (note that I_{ext} comes from a Gaussian distribution, see Section 2.1) below a threshold and these cells often fire single spikes (Fig. 7E) rather than clusters (Fig. 7F).

The phase delay between the GABAergic and the glutamatergic cells (Fig. 8A) reflects the time required to the activation of the GABAergic cells. The phase delay of the *ISP* relative to the *ESP* is higher than 180° (Fig. 8A) because the neurons of the *ISP* do not have a phasic excitatory drive. Cells with lower firing rate fire later in both SPs (Fig. 8B, C). The phase difference between the two SPs decreased if the external current or the strength of the glutamatergic innervation of the *ESP* was increased (Fig. 8D, E). It also showed a small decrease if the GABAergic innervation of the *ISP* was stronger (the bias is positive on Fig. 8F). All of these changes enhanced the phasic inhibition of the *ISP* and enlarged the gap between the activation of the two SPs (see shaded box on Fig. 6C, D). When the bias of the synaptic connections is high the circuit is similar to a feed-forward network, where the glutamatergic cells form the first layer and the *ESP* and the *ISP* the second and the third one, respectively. The phase difference was independent of the polarization of the network (Fig. 8G). No phase difference larger than ∼160° was observed between the *ESP* and the *ISP*. This is due to the fact that an increased phase difference could be brought about by decreased I_{ext} and/or decreasing the strength of the glutamatergic innervation but such decrease over a certain limit (corresponding to ∼160° phase difference) would make one of the SPs silent.

4. Discussion and conclusions

In this section we will compare the two models with each other and with experimental findings. Table 1 showing the

Table 1 The similarities and the differences between the two models

Phenomenon	Ping-Pong model	Feed-forward model
Theta in medial septal slice is	possible	possible
GABAergic cells in the MSDB fire theta periodic clusters	*in vivo* and *in vitro*	*in vivo*
GABAergic neurons are *in vitro*	cluster-firing cells	fast-firing cells
Theta periodicity in GABAergic cells is caused by	a slow potassium current	synaptic input
Firing rate of neurons can be different	slightly (10−25 Hz)	largely (5−45 Hz)
Firing rate and preferred firing phase	no correlation	cells with lower firing rate fire later
Cells are synchronized through	GABAergic	glutamatergic and GABAergic synapses
The network structure required for synchronization	polarized network of GABAergic neurons	random network of glutamatergic and GABAergic neurons, glutamatergic neurons innervate a proportion of GABAergic cells
Phase distribution of GABAergic neurons	bimodal (150−180°)	bimodal (120−150°) or unimodal
Locale application of glutamate antagonist	has no effect	disrupt hippocampal and septal theta oscillation
Locale application of GABA antagonist	desynchronizes clustering cells	no effect/disrupts clustering activity

similarities and the differences between the two models serves as an ordered summary for the following paragraphs.

4.1. Electrophysiology of the MSDB

Experimental evidence underly that periodic firing of MSDB neurons *in vivo* remain after chronic isolation from the brainstem or from the hippocampus (Vinogradova et al., 1980; Vinogradova, 1995). These results suggest that neurons in the MSDB can act as autonomous pacemaker. Indeed, coherent extracellular oscillation at theta frequency in the MSDB slice preparation was observed in the presence of kainate, a glutamate receptor agonist (Garner et al., 2005). However, in this study putative GABAergic and cholinergic neurons fired single action potentials in each theta cycle rather than clusters. In another study Manseau et al. (2005) observed synchronized glutamatergic bursts under epileptogen conditions *in vitro* in various cell types in the MSDB. Although the frequency was much slower and the duration of these bursts was much longer than under *in vivo* conditions, it is remarkable that in both studies the synchronized activity in the MSDB is linked to the activation of glutamatergic receptors as in our feed-forward model. These experimental results served as rationale on which we based the hypothesis that intraseptal mechanisms alone might serve as generators of the theta pacemaker activity and proposed models that are in accordance with the above observations.

Contrary to *in vitro* preparations where cholinergic and GABAergic cells exhibit slow-firing and fast-firing activity, respectively (Griffith and Matthews, 1986; Morris et al., 1999; Knapp et al., 2000) both cholinergic and GABAergic cells were found to display burst-firing activity *in vivo* (King et al., 1998; Brazhnik and Fox, 1999). Moreover, further studies (Griffith, 1988; Griffith et al., 1991; Henderson et al., 2001; Sotty et al., 2003) underpin the notion that under *in vitro* conditions medial septal cells do not exhibit sustained cluster- or burst-firing activity in the theta frequency range. Following this line of thoughts, we might conclude that there exist some conditions favoring burst-firing *in vivo*, which have not been reproduced *in vitro* yet. In the presented computer simulations we experiment with changing the firing characteristics of different cell types (GABAergic and glutamatergic) and conclude that in the studied situations even if GABAergic cells are not cluster-firing cells they can exhibit clustering properties, which could explain the apparent duality of GABAergic cell firing properties *in vivo* and *in vitro*.

Arrangement of spikes in theta periodic clusters can rely both on intrinsic or extrinsic mechanisms. A specific ion channel might serve as the basis of a mechanism of intrinsic theta modulation of activity as in our modeled cluster-firing cell. Like the regulation of the H-current is mediated by metabotropic receptors via the intracellular concentration of the cyclic AMP (Wainger et al., 2001), the regulation of an ion channel responsible for cluster-firing behavior may require specific extracellular environment (e.g. neuromodulators from the brainstem) that is not present *in vitro*. Interaction between neurons through synapses can also results in a rhythmic firing pattern as in our feed-forward model. In this case modulation of the fast synaptic dynamics causes a substantial change in the firing pattern of the neurons (see further discussion in Section 4.3 and 4.4).

Heterogeneity in their firing rate is a prominent characteristic of medial septal neurons (King et al., 1998; Brazhnik and Fox, 1999; Dragoi et al., 1999; Bor-hegyi et al., 2004) *in vivo*. This heterogeneity is present in both of our models, but the mean firing rate is lower in the ping-pong model (similar to Bor-hegyi et al. (2004)) and higher in the feed-forward model (like in King et al. (1998); Brazhnik and Fox (1999)).

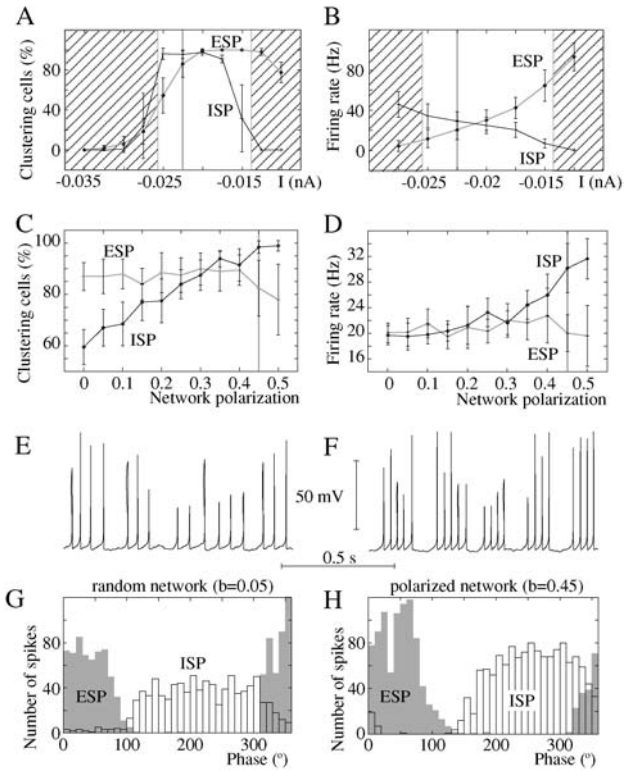

Fig. 7 Change in the external current but not in the network structure disrupts coherent oscillation in the fast-firing GABAergic network. A–B: When the external current applied to the *ESP* is in the $-0.025 \leq I_{\text{ext,ESP}} \leq -0.0175$ nA range the proportion of clustering cells (A) is high and the firing rate of the two subpopulations are similar (B) in the two subpopulations ($I_{\text{ext,ISP}} = -0.012$ nA, bias $= 0.45$). Vertical gray lines indicate the default parameter values used in the feed-forward model, while shaded regions mark physiologically non-relevant parameter ranges. C–F: Change in the bias does not alter the activity of the *ESP* because of its strong glutamatergic drive (C–D: gray lines, $I_{\text{ext,ESP}} = -0.0225$ nA). Cells with lower firing rate (E, ∼17 Hz) do not show clustering behavior like cells with higher firing rate (F, ∼22 Hz) (both cells shown in E and F are from the *ISP*). Since more cells fire at lower frequency due to denser feed-back inhibition in random than in polarized networks, the mean firing rate (D, black line) and the number of clustering neurons (C, black line) in the *ISP* are lower in random networks than in polarized networks. G-H: The phase distribution of spikes in the random (G) and in the polarized networks (H) for *ESP* (gray) and *ISP* (black), respectively

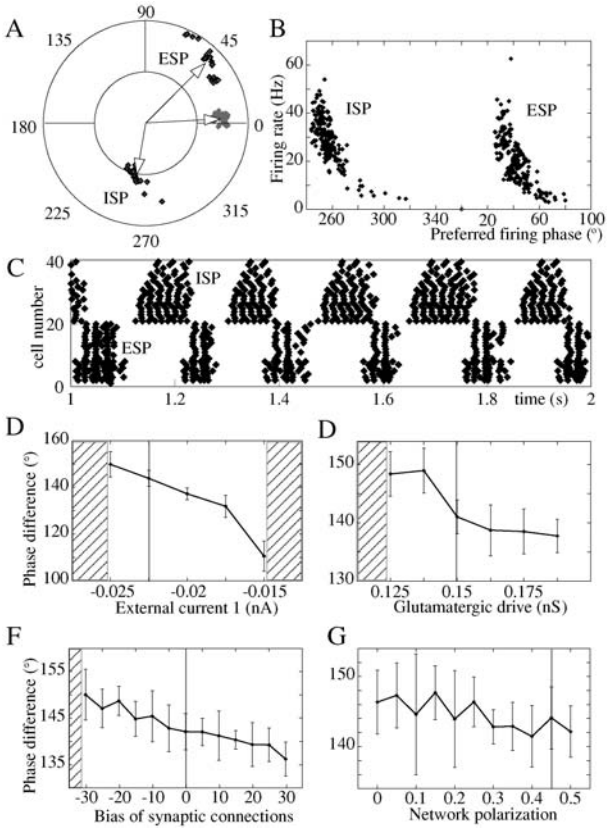

Fig. 8 Phase relationships in the feed-forward model A: Polar plot shows the phase relationship between glutamatergic (gray dots) and GABAergic (black dots) cells. Cells from the *ESP* have a slight phase delay (∼45°) relative to the glutamatergic cells. Cells from *ISP* have a phase delay more than ∼180° relative to cells from *ESP* due to their delayed activation (see Fig. 6C, D). B: Correlation between the firing rate and the preferred firing phase was significantly negative (for the *ESP*: −0.53; for *ISP*: −0.75). C: Neurons on the raster plot are ordered according to their preferred firing phase. Cells with smaller number (earlier phase) usually have higher firing rate within the SP. D–G: The phase difference between the two subpopulations depends on the external current applied to the *ESP* (D), the strength of the glutamatergic input (E), the bias of the strength of GABAergic synapses (F). Bias is the difference from the mean synaptic conductance in %. It is positive if the synaptic connections from *ESP* to *ISP* are stronger than from *ISP* to *ESP*. The phase difference was independent from the polarization of the network (G) and was always smaller than ∼160°. Vertical gray lines indicate the default parameter values used in the feed-forward model, while shaded regions mark physiologically non-relevant parameter ranges

The firing rate of a neuron can be varied in a wider range in the feed-forward model because in the ping-pong model the membrane dynamics do not permit cluster-firing with firing rates higher than ∼40 Hz.

Bor-hegyi et al. (2004) found that cells with longer bursts tended to fire around the peak while short burst neurons fired around the trough of the hippocampal theta. Our models can reproduce this finding when the external current of the two SPs are different (Fig. 8C). Correlation between the firing rate and the preferred firing phase characterize neurons within one SP in our feed-forward model, whereas no such correlation was found in the ping-pong model. This correlation has not been studied yet experimentally.

4.2. Network structure and preferred firing phase

A specific network structure is required for synchronization of GABAergic neurons in our ping-pong model. Recent anatomical studies (Henderson et al., 2004) revealed two PV+ cell populations in the medial septum: one medially

and another more laterally located. These two populations differ in their GABAergic innervation: PV+ basket-like terminals are on medially located cells, while there are fewer PV+ synapses on the laterally located neurons. It is possible that these parvalbumin-positive populations correspond to the two, antiphasically oscillating cell-populations described by Bor-hegyi et al. (2004). In the same study Henderson et al. (2004) filled a fast-spiking, putative PV+ neurons with biocitin and found that their synaptic contacts with other PV+ neurons were similar to that described above. However, they did not determine if PV+ contacts on the biocitin filled neurons were basket-like or not. If a neuron having basket-like contacts on its soma do not form basket-like synapses on other neurons and vice versa that would be a direct evidence for the presence of a polarized network of GABAergic neurons in the medial septum, which is crucial to synchronization in our ping-pong model.

Brazhnik and Fox (1997) found that theta periodic membrane oscillation of brief-spike (putative GABAergic) cells is mediated by glutamatergic EPSPs, while rhythmic firing of long-spike (putative cholinergic) cells are driven by GABAergic IPSPs. These two populations fired in the opposite phase of the dentate theta. They suggested a feed-forward network where GABAergic neurons are driven by glutamatergic EPSPs and they provide phasic inhibition to cholinergic neurons. Later (Brazhnik and Fox, 1999) they also showed that intraseptal blockade of GABAergic transmission eliminated rhythmicity of putative cholinergic cells, whereas rhythmicity of putative GABAergic neurons remained unchanged. In our feed-forward model when the bias of synapses is positive (Fig. 8E) the *ISP* could be replaced with a population of cholinergic neurons as Brazhnik and Fox (1999) suggest. In this case, if we accept that only one GABAergic population is present in the MSDB then the phase distribution of GABAergic neurons will be unimodal. Contrary to this, Henderson et al. (2004) did not find parvalbumin containing terminals on the somata of the cholinergic cells in the MSDB, however, it is also possible that not all septal GABAergic neuron contain parvalbumin.

GABAergic neurons identified by their parvalbumin immunoreactivity form two distinct populations according to their preferred firing phases relative to the hippocampal theta oscillation (Bor-hegyi et al., 2004). Other studies classifying GABAergic and cholinergic cells based on the shape of the action potential found that putative GABAergic cells show unimodal phase distribution (Brazhnik and Fox, 1997) or no phase preference (King et al., 1998) related to the hippocampal theta. However, these cells were shown to be ChAT negative (Griffith, 1988) but no GABAergic marker was tested, therefore they can be either glutamatergic or GABAergic neurons. If the glutamatergic neurons and the two GABAergic populations of our feed-forward model are taken together we get three distinct peaks located on one side of the phase-circle (Fig. 8A). In experiments the average firing phase of these three populations measured together would result in a similar phase distribution as found by Brazhnik and Fox (1999).

4.3. Pharmacological modulation of the septal theta rhythm

Pharmacological modification of synapses among the medial septal neurons offers to be a possible tool to reveal the network connectivity. Synaptic connections may play an important role in modifying the firing pattern of a given cell or in the synchronization of two neurons. Physiological evidences suggest that rhythmic burst-firing of different neurons in the medial septum rely on phasic activation through cholinergic, GABAergic and glutamatergic synaptic connections (Stumpf et al., 1962; Stewart and Fox, 1989; Brazhnik and Fox, 1997).

Brazhnik and Fox (1999) found that local injection of scopolamine (a cholinergic antagonist) abolishes the burst-firing activity of cholinergic but not that of putative GABAergic neurons in anaesthetized rats. In freely moving rats, however, scopolamine decreased the firing rate of both cholinergic and GABAergic neurons. The $GABA_A$ antagonist picrotoxin also disrupts burst-firing activity of cholinergic but not GABAergic neurons in freely moving rat. Preferred firing phase of these neurons were stable under drug application. Taken together, it is unlikely that rhythmic firing of GABAergic neurons is the effect of GABAergic or cholinergic synaptic modulation.

Blocking the GABAergic synapses in our ping-pong model causes desynchronization of these neurons but the cells remain theta periodic. However, a feed-back from the hippocampus is able to maintain synchronized activity of the network like in the study of Wang (2002). GABAergic blockade in our feed-forward model abolishes theta periodic firing of GABAergic neurons from the *ISP*.

4.4. Glutamatergic neurons

The robust in phase synchronization of glutamatergic cells in our model raise the possibility that this circuit can serve as theta periodic pacemaker for septal and also for hippocampal neurons.

Blocking AMPA receptors in the medial septum does not abolish hippocampal theta in the behaving rat (Leung and Shen, 2004) but under urethane anaesthesia local infusion of AMPA receptor antagonists to the MSDB disrupt hippocampal theta oscillation triggered by intraseptal cholinergic activation (Puma and Bizot, 1999). These studies suggest that glutamatergic neurons are involved in the generation of the atropine sensitive theta in the hippocampus.

Manseau et al. (2005) observed large glutamatergic bursts in various cell types including putative glutamatergic neurons. These neurons fired clusters of action potentials in response to constant depolarization but in the presence of 4-AP (a potassium channel blocker) and bicuculline (a $GABA_A$ antagonist) they fired bursts on the top of a large excitatory wave. The frequency of the bursts were much slower than the frequency of the theta oscillation. Their study suggests that glutamatergic neurons are able to pace synchronized rhythmic activity in the MSDB. On the other hand, these experiments did not explain how large excitatory bursts could emerge in a network of cluster-firing neurons.

The effect of local application of glutamate receptor antagonists to the firing pattern of MSDB neurons have not been studied. Our feed-forward model predicts that the local application of an AMPA receptor antagonist would result in desynchronization of glutamatergic cells and would disrupt clustering activity of GABAergic neurons. However, if hippocampal theta remains after the drug injection a feed-back from the hippocampus may also be able to maintain synchronized burst-firing activity in a part of the network.

4.5. Conclusions and main results

We gave two different models to describe the generation of synchronized theta activity in medial septal GABAergic networks. An important characteristic of both models is that the GABAergic neurons are able to fire synchronized clusters of action potentials in the absence of periodic input from another brain area. This means that if GABAergic cells are cluster firing and their connections in the MSDB are organized similarly to the proposition of the ping-pong model then septal GABAergic cells are able to pace other brain regions by themselves. If, on the other hand, they rather have fast-firing characteristics one way to elicit clustering behavior is to provide these cells with phasic input. One possible source of such an input, as shown in the feed-forward model, is a network of local cluster-firing glutamatergic cells.

Both of our models were inspired by the recent experiment of Bor-hegyi et al. (2004) showing that parvalbumin containing GABAergic cells show bimodality in their preferred firing phase distribution. Both of our models were designed to reproduce this property.

We also showed that non-cluster-firing cells when connected in an appropriate network (e.g. similar to the one sketched in the feed-forward model) show clustering behavior due to emergent network dynamics. This finding might help to understand why *in vivo* and *in vitro* experiments characterize differently the firing properties of a given cell type.

Furthermore, our computer simulations show that a local network of interconnected glutamatergic cluster-firing neurons in the MSDB is able to generate robust theta periodic drive to GABAergic neurons.

Appendix

Membrane potential change of the cluster-firing model taken from Wang (2002) is given by the following current balance equation:

$$C_m dV/dt = -I_{Na} - I_K - I_{KS} - I_L - I_{syn} + I_{extx} \qquad \text{(A-1)}$$

where $C_m = 1\mu$ F/cm^2, I_{syn}, the synaptic and I_{ext}, the external currents are described in the Methods section. The leakage current is described by the following equation: $I_L = (V - E_L)/R_m$ where $R_m = 1\,\Omega/m^2$ and $E_L = -50$ mV.

The three voltage-dependent currents were described by the Hodgkin-Huxley formalism where the gating variable x satisfies a first order kinetics: $dx/dt = \alpha_x(V)(1-x) - \beta_x(V)x \equiv (x_{inf}(V) - x)/\tau_x(V)$. The sodium current ($I_{Na}$) was in the standard form:

$$I_{Na} = g_{Na} m_{inf}^3 n(V - E_{Na}) \qquad \text{(A-2a)}$$

$$m_{inf} = \alpha_m/(\alpha_m + \beta_m) \qquad \text{(A-2b)}$$

$$\alpha_m = -10^2 \cdot (V + 0.033)/(\exp(-10^2 \cdot (V + 0.033)) - 1) \qquad \text{(A-2c)}$$

$$\beta_m = 4 \cdot \exp(-(V + 0.058)/0.018) \qquad \text{(A-2d)}$$

$$\alpha_h = \phi \cdot 70 \cdot \exp(-(V + 0.051)/0.010) \qquad \text{(A-2e)}$$

$$\beta_h = \phi \cdot 10^3/(\exp(-10^2 \cdot (V + 0.021)) + 1) \qquad \text{(A-2f)}$$

The delayed rectifier potassium current (I_K) was described as:

$$I_K = g_K n^4 (V - E_K) \qquad \text{(A-3a)}$$

$$\alpha_n = (-\phi \cdot 10^4 \cdot (V + 0.038))/(\exp(-10^2 \cdot (V + 0.038)) - 1) \qquad \text{(A-3b)}$$

$$\beta_n = 125 \cdot \phi \cdot \exp(-(V + 0.048)/0.080) \qquad \text{(A-3c)}$$

The slow potassium current (I_{KS}):

$$I_{KS} = g_{KS} pq(V - E_K) \qquad \text{(A-4a)}$$

$$p_{\text{inf}} = 1/(1 + \exp(-(V + 0.034)/0.0065)) \quad \text{(A-4b)}$$

$$q_{\text{inf}} = 1/(1 + \exp((V + 0.065)/0.0066)) \quad \text{(A-4c)}$$

$$\tau_{\text{q}} = \tau_{\text{q0}} \cdot (1 + 1/(1 + (\exp -(V + 0.05)/0.0068))) \quad \text{(A-4d)}$$

with parameters $\tau_{\text{p}} = 6$ s, $\tau_{\text{q0}} = 0.1$ s.

The maximal conductance and the reversal potential of the ion channels were set as follows: $g_{\text{Na}} = 500$ S/m^2, $g_{\text{K}} = 80$ S/m^2, $g_{\text{KS}} = 120$ S/m^2; $E_{\text{Na}} = 55$ mV, $E_{\text{K}} = -85$ mV. The membrane surface was taken to be 1.26×10^3 mm^2, equivalent to the surface area of a sphere of 20 μm diameter.

To model the MSDB fast-firing neurons we simplified the cluster-firing model by omitting the term I_{KS} from equation A-1, and changing the ϕ parameter in equation A-2e –f and A-3b–c from 5 to 10.

Acknowledgments Authors are greatly thankful for Péter Érdi for invaluable discussions both in Kalamazoo and Csillebérc. Also thank to Mihály Hajós for his inspiring experiments. This project was supported by the Henry R. Luce Foundation, the National Scientific Research Foundation, OTKA (grant no: T038140) and the ICEA project (EU FP6 Programme, grant no.: IST-4-027819-IP).

References

Bland BH, Oddie SD, Colom, LV (1999) Mechanisms of neural synchrony in the septohippocampal pathways underlying hippocampal theta generation. J. Neurosci. 19(8): 3223–3237.

Bor-hegyi Z, Varga V, Szilágyi N, Fabó D, Freund TF (2004) Phase segregation of medial septal GABA ergic neurons during hippocampal theta activity. J. Neurosci. 24(39): 8470–8479.

Bower JM, Beeman D (1998) The Book of GENESIS: Exploring Realistic Neural Models with the GEneral NEural SImulation System, 2 edition. Springer–Verlag.

Brashear HR, Zaborszky L, Heimer L (1986) Distribution of GABAergic and cholinergic neurons in the rat diagonal band. Neuroscience 17(2): 439–451.

Brazhnik ES, Fox SE (1997) Intracellular recordings from medial septal neurons during hippocampal theta rhythm. Exp. Brain. Res. 114(3): 442–453.

Brazhnik ES, Fox SE (1999) Action potentials and relations to the theta rhythm of medial septal neurons *in vivo*. Exp. Brain Res. 127(3): 244–258.

Cole AE, Nicoll RA (1984) Characterization of a slow cholinergic post-synaptic potential recorded *in vitro* from rat hippocampal pyramidal cells. J. Physiol. 352: 173–188.

Colom LV, Castaneda MT, Reyna T, Hernandez S, Garrido-Sanabria E (2005) Characterization of medial septal glutamatergic neurons and their projection to the hippocampus. Synapse 58(3): 151–164.

Destexhe A (2000) Modelling corticothalamic feedback and the gating of the thalamus by the cerebral cortex. J. Physiol. (Paris) 94: 391–410.

Dragoi G, Carpi D, Recce M, Csicsvári, J, Buzsáki G (1999) Interactions between hippocampus and medial septum during sharp waves and theta oscillation in the behaving rat. J. Neurosci. 19: 6191–99.

Dayan P. Abbott L (2001) Theoretical Neuroscience: Computational and Mathematical Modeling of Neural Systems. MIT Press. Chapter 1: Neural encoding: Firing rates and spike statistics.

Ermentrout B (2002) Simulating, Analyzing, Animating Dynami cal Systems: A Guide to XPPAUT for Researchers and Students. SIAM, Philadelphia, PA.

Freund TF (1989) GABAergic septohippocampal neurons contain parvalbumin. Brain Res. 478(2): 375–381.

Freund TF, Antal M (1988) GABA-containing neurons in the septum control inhibitory interneurons in the hippocampus. Nature 336(6195): 170–173.

Frotscher M, Leranth C (1985) Cholinergic innervation of the rat hippocampus as revealed by choline acetyltransferase immunocytochemistry: A combined light and electron microscopic study. J. Comp. Neurol. 239(2): 237–246.

Garner HL, Whittington MA, Henderson Z (2005) Induction by kainate of theta frequency rhythmic activity in the rat medial septum-diagonal band complex *in vitro*. J. Physiol. 564(Pt 1): 83–102.

Green JD, Arduini AA (1954) Hippocampal electrical activity in arousal. J. Neurophysiol 17: 533–557.

Griffith W (1988) Membrane properties of cell types within guinea pig basal forebrain nuclei *in vitro*. J. Neurophysiol 59(5): 1590–1612.

Griffith W Matthews R (1986) Electrophysiology of AChE-positive neurons in basal forebrain slices. Neurosci. Lett. 71(2): 169–174.

Griffith W, Sim J, Matthews R (1991) Electrophysiologic characteristics of basal forebrain neurons *in vitro*. Adv. Exp. Med. Biol. 295: 143–155.

Hajszan T, Alreja M, Leranth C (2004) Intrinsic vesicular glutamate transporter 2-immunoreactive input to septohippocampal parvalbumin-containing neurons: Novel glutamatergic local circuit cells. Hippocampus 14(4): 499–509.

Hasselmo ME, Hay J, Ilyn M, Gorchetchnikov A (2002) Neuromodulation, theta rhythm and rat spatial navigation. Neural Netw. 15(4–6): 689–707.

Henderson Z, Fiddler G, S Saha AB, Halasy K (2004) A parvalbumin-containing, axosomatic synaptic network in the rat medial septum: relevance to rhythmogenesis. Eur. J. Neurosci. 19(10): 2753–2798.

Henderson Z, Morris N, Grimwood P, Fiddler G, Yang H, Appenteng K (2001) Morphology of local axon collaterals of electrophysiologically characterised neurons in the rat medial septal/diagonal band complex. J. Comp. Neurol. 430(3): 410–432.

King C, Recce M, O'Keefe J (1998) The rhythmicity of cells of the medial septum/diagonal band of broca in the awake freely moving rat: Relationships with behaviour and hippocampal theta. European J. Neurosci. 10: 464–477.

Kiss J, Patel AJ, Baimbridge KG, Freund TF (1990) Topographical localization of neurons containing parvalbumin and choline acetyltransferase in the medial septum-diagonal band region of the rat. Neuroscience 36(1): 61–72.

Knapp J, Morris N, Henderson Z, Matthews R (2000) Electrophysiological characteristics of non-bursting, glutamate decarboxylase messenger RNA-positive neurons of the medial septum/diagonal band nuclei of guinea-pig and rat. Neuroscience 98(4): 661–668.

Lengyel M, Huhn Z, Erdi P (2005) Computational theories on the function of theta oscillations. Biol. Cybern. 92(6): 393–408.

Leung L, Shen B (2004) Glutamatergic synaptic transmission participates in generating the hippocampal EEG. Hippocampus. 14(4):510–525.

Manseau F, Danik M, Williams S (2005) A functional glutamatergic neurone network in the medial septum and diagonal band area. J. Physiol. 566(3): 865–884.

Morris NP, Harris SJ, Henderson Z (1999) Parvalbumin-immunoreactive, fast-spiking neurons in the medial septum/diagonal band complex of the rat: Intracellular recordings *in vitro*. Neuroscience 92(2): 589–600.

O'Keefe J. and Nadel L (1978) The Hippocampus as a Cognitive Map. Clarendon Press, Oxford.

Petsche H, Stumpf C ,Gogolak G (1962) The significance of the rabbit's septum as a relay station between the mid-brain and the hippocampus. I The control of hippocampal arousal activity by the septum cells. Electroencephalogr. Clin. Neurophysiol. 14: 202–211.

Puma C, Bizot JC (1999) Hippocampal theta rhythm in anesthetized rats: Role of AMPA glutamate receptors. Neuroreport 10(11): 2297–2300.

Serafin M, Williams S, Khateb A, Fort P, Muhlethaler M (1996) Rhythmic firing of medial septum non-cholinergic neurons. Neuroscience 75(3): 671–675.

Sotty F, Danik M, Manseau F, Quirion R, Williams S (2003) Distinct electrophysiological properties of glutamatergic, cholinergic and GABAergic rat septohippocampal neurons: Novel implications for hippocampal rhythmicity. J. Physiol. 551: 927–943.

Stewart M, Fox, SE (1989) Two populations of rhythmically bursting neurons in rat medial septum are revealed by atropine. J. Neurophysiol. 61(5): 982–993.

Stewart M, Fox SE (1990) Do septal neurons pace the hippocampal theta rhythm?Trends Neurosci. 13(5): 163–168.

Stumpf C, Petsche H, Gogolak G (1962) The significance of the rabbit's septum as a relay station between the midbrain and the hippocampus. II. The differential influence of drugs upon both the septal cell firing pattern and the hippocampus theta activity. Electroencephalogr. Clin. Neurophysiol. 14: 212–219.

Vanderwolf CH (1969) Hippocampal electrical activity and voluntary movement in the rat. Electroencephalogr. Clin. Neurophysiol. 26(4): 407–418.

Vértes RP, Kocsis B (1997) Brainstem-diencephalo-septohippocampal systems controlling the theta rhythm of the hippocampus. Neuroscience 81: 893–926.

Vinogradova O, Brazhnik E, Karanov A, Zhadina S (1980) Neuronal activity of the septum following various types of deafferentation. Brain Res. 187(2): 353–368.

Vinogradova OS (1995) Expression, control, probable functional significance of the neuronal theta-rhythm. Prog. Neurobiol. 45(6): 523–583.

Wainger B, DeGennaro M, Santoro B, Siegelbaum S, Tibbs G (2001) Molecular mechanism of cAMP modulation of HCN pacemaker channels. Nature 411(6839): 805–10.

Wang XJ (2002) Pacemaker neurons for the theta rhythm and their synchronization in the septohippocampal reciprocal loop. J. Neurophysiol. 87(2): 889–900.

Wang XJ, Buzsáki G (1996) Gamma oscillation by synaptic inhibitionin a hippocampal interneuronl network model. J. Neurosci. 16: 6402–6413.